

## Optical Properties of Polymer Films for Transparent Insulation

Gernot M. Wallner<sup>1\*</sup>, Reinhold W. Lang<sup>1,2</sup>, Werner Platzer<sup>3</sup>, Christian Teichert<sup>4</sup>

<sup>1</sup>Institute of Materials Science and Testing of Plastics, University of Leoben, Franz-Josef-Str. 18, 8700 Leoben, Austria

<sup>2</sup>Institute of Polymer Technology, JOANNEUM RESEARCH Forschungsges.m.b.H., Leoben, Austria

<sup>3</sup>Fraunhofer-Institute for Solar Energy Systems, Freiburg, Germany

<sup>4</sup>Institute of Physics, University of Leoben, Austria

**Summary:** Commercially available, highly transparent polymer films for transparent insulation applications were investigated systematically as to their relevant optical properties in the solar and infrared wavelength range. The photometric characterisation in the solar range and the calculation of non-spectral, solar optical film properties using models for scattering-absorbing media have shown, that the solar extinction is dominated by scattering occurring mainly at the surface. For various amorphous and semi-crystalline films the root-mean-square surface roughness correlated well with the solar optical thickness. Regarding high infrared absorptance in the wavelength range of about 10  $\mu\text{m}$  the carbon-oxygen single bond is highly effective for commercial materials with maximum service temperatures of about 100 °C. For 50  $\mu\text{m}$  thick films of different polymer types with carbon-oxygen single bonds in the molecular structure a good correlation between the concentration of the functional carbon-oxygen group and the non-spectral, infrared optical thickness was found.

### Introduction

Due to their excellent optical properties (high transparency) and thermal characteristics (low heat conductivity) as well as further polymer-specific advantages (e.g., material properties which can be varied within a wide range; highly flexible processability; high economy) polymer films possess an outstanding potential for many solar applications. At present transparent polymer films are already used for encapsulation of photovoltaic (PV) cells, as convection barrier in solar collectors and as substrate or adhesive layer for glazings. Previous research on solar and infrared optical properties of films focused on selected polymer types or selected radiation ranges and properties.<sup>[1–3]</sup> However, so far no comprehensive investigations have been reported which systematically consider the effects of polymer structure and morphology and the film thickness on the averaged optical properties in the solar and medium infrared range.

Hence, the purpose of this paper is to describe and compare the results obtained for solar

optical and infrared optical properties of various commercial polymer films. In particular, the effects of polymer structure, morphology and film thickness on the integral optical properties with the specific view on the use of such polymer films in transparent insulation (TI)<sup>[1, 4, 5]</sup> structures will be discussed. The results are interpreted in terms of both the molecular and supermolecular structure of the various polymer film types.

## Background and Methodology

To develop and optimize transparent insulation (TI) structures based on polymer films properly it was necessary to investigate polymer films as to their relevant integral optical properties (solar scattering coefficient,  $\sigma^S$ ; solar absorption coefficient,  $\kappa^S$ ; infrared absorption coefficient,  $\kappa_{IR}$ ). First, a market survey was carried out on commercially available transparent polymer films. In total, more than 80 different polymer films with thicknesses ranging from 12 to 150  $\mu\text{m}$  were selected for the investigations. As to the influence of film thickness, care was taken to select film types, which were processed from the same moulding compound.

All polymer films were characterized spectroscopically at normal or near-normal incidence and the integral values were calculated based on published theories and formulas. Values for film thickness and the index of refraction over the whole radiation range were taken from data sheets and from the literature. In addition, the thickness of all films was measured with a caliper.

To establish structure-property-correlations in the solar wavelength range the surface topography of selected polymer films was characterized by Atomic Force Microscopy (AFM); recording scans in an appropriate bandpass the roughness parameters were determined quantitatively. In the infrared wavelength range the optical properties were correlated to the molecular structure of the investigated polymers.

## Experimental and Calculation Procedures

The polymer films investigated included commodity and technical polymers with maximum service temperatures of about 100 °C (e.g., polypropylene (PP), polymethylpentene (PMP), polymethylmethacrylate (PMMA), polyethyleneterephthalate (PET), polycarbonate (PC), cellulose acetate (CA; degree of substitution: 2.5)) as well as high temperature resistant polymers such as ethylene-tetrafluorethylene copolymer

(E/TFE), tetrafluorethylene-perfluoropropylene copolymer (F/EP), polyetheretherketone (PEEK), polyetherimide (PEI) or polysulfone (PSU). Relevant information as to the material supplier, the polymer morphology (amorphous or semi-crystalline), the polymer structure, the index of refraction, the film thicknesses and the production process are summarized in ref. [6].

The optical data used for inputs to the calculations were determined using two experimental techniques. Over the solar spectrum from 300 to 2500 nm the collimated-hemispherical (i.e., total transmitted radiance at beam irradiance) and collimated-diffuse (i.e., diffuse transmitted radiance at beam irradiance) transmittance values at normal incidence and reflectance values at near-normal incidence were determined using a Perkin Elmer Lambda 9 Ulbricht sphere spectrophotometer (Perkin Elmer, Überlingen, Germany). The BaSO<sub>4</sub> coated Ulbricht sphere had a diameter of 15 cm. For the given measurement apparatus the radiation passing through the specimen or being reflected by the specimen outside a cone of approximately 5° relative to the incident beam direction is defined as diffuse component. The hemispherical and diffuse values allowed the calculation of both, the extinction coefficient due to absorption and the scattering coefficient.

Over the medium IR range from 180 to 4000 cm<sup>-1</sup> (2.5 to 55.5 μm) the collimated-collimated (i.e., beam transmitted radiance at beam irradiance) transmittance spectra at normal incidence were obtained with a Perkin Elmer PE330 grating spectrophotometer (Perkin Elmer, Überlingen, Germany). Thus, the Planck radiation of a body at ambient temperature was covered to approximately 98 %.

To calculate the integral solar absorption coefficient,  $\kappa^S$ , and the scattering coefficient,  $\sigma^S$ , at first the spectral collimated and diffuse transmittance and reflectance data were averaged by weighting the measured spectral data by the AM 1.5 Global solar irradiance source function. These experimental integral properties were input data for a optimization routine. The 4-flux model (a generalization of the Maheu model<sup>[7]</sup>) was used to calculate theoretical transmittance and reflectance values as a function of the integral absorption and scattering coefficients. Further details on relevant assumptions necessary for the 4-flux model are described in ref. [6]. The 4-flux model calculations gave theoretical values for the following four parameters: collimated-collimated transmittance,  $\tau_{cc}$ , collimated-diffuse transmittance,  $\tau_{cd}$ , collimated-collimated reflectance,  $\rho_{cc}$ , and collimated-diffuse reflectance,  $\rho_{cd}$ . Subsequently, the error function,

that is the sum of the square of the difference between experimental and theoretical values, was minimized and the variables  $\kappa^S$  and  $\sigma^S$  were optimized numerically. As starting parameters the absorption coefficient was defined as 0, and the scattering coefficient was set equal or larger than the overall extinction coefficient calculated from the experimental  $\tau_{cc}$  value.

To determine the integral infrared absorption coefficient,  $\kappa_{IR}$ , at first the directional spectral absorptance,  $\alpha_\lambda(\theta)$ , was calculated for both transverse electric and transverse magnetic polarization using the spectral collimated-collimated transmittance, the film thickness and a constant index of refraction from the visible range as input parameters according to Rubin.<sup>[2]</sup> The hemispherical spectral absorptance,  $\alpha_{\lambda,h}$ , for unpolarized radiation was found by numerical integration over the hemisphere in steps of 5 degrees and averaging over both polarization directions. Finally, the total hemispherical absorptance,  $\alpha_h(T)$ , was determined by averaging the spectral values, weighted by a blackbody emissive power,  $P(\lambda,T)$ , at each wavelength. The effective temperature dependent absorption coefficient,  $\kappa_{IR}(T)$ , was found by an inverse fit. Although  $\kappa_{IR}$  in general is temperature dependent, in this paper the absorption coefficient,  $\kappa_{IR}$ , for 20 °C only is described and discussed, as this temperature is of special relevance for TI wall applications.

To characterize the surface topography of selected films AFM was performed in tapping mode (frequency: 250 to 300 kHz) using a NanoScope MultiMode™ Atomic Force Microscope (Digital Instruments, Santa Barbara, CA, USA). Images were recorded under ambient conditions using commercially fabricated Si tips with radii between 5 and 10 nm. To allow comparison with the solar optical scattering properties 50  $\mu\text{m}$  x 50  $\mu\text{m}$  scans were run (bandpass: 100 nm to 50  $\mu\text{m}$ ). The relevant roughness parameters (i.e., root-mean-square roughness,  $\sigma$ , lateral correlation length,  $\xi$ , roughness exponent,  $\alpha$ ) were calculated analyzing one dimensional cross-sections of the height images.<sup>[8]</sup>

## Results and Discussion

In the following the solar and infrared optical properties will be described and discussed separately. Due to restrictions in space only selected data sets are presented, which, however, are representative of the various molecular and microstructural effects observed.

## Solar Optical Properties

The collimated-hemispherical and collimated-diffuse transmittance and reflectance spectra for 50  $\mu\text{m}$  thick films of PC and E/TFE are shown in Figure 1. The different collimated-hemispherical transmittance,  $\tau_{\text{ch}}$ , and reflectance,  $\rho_{\text{ch}}$ , values are a result of the different indices of refraction, which are 1.59 and 1.40 for PC and E/TFE, respectively. Due to dispersion effects the  $\tau_{\text{ch}}$  values are slightly decreasing and the  $\rho_{\text{ch}}$  values are slightly increasing at shorter wavelengths. In the near UV range (300 to 400 nm), PC shows a pronounced absorption which can be attributed to electron excitations in interatomic bonds (e.g., double bonds of aromatic ring structures and the carbonyl groups of the polymer chain and/or various bonds of the light stabilizer molecules). While the investigated PC grade contained a UV stabilizer, for E/TFE (which is inherently light stable and thus contains no light stabilizer) the near UV absorption phenomena are not detected as the bonds of E/TFE do not absorb in the investigated UV range. Moreover, in the near IR range PC shows moderate absorptions due to vibration activations of C-H and C=O bonds. As the C-F bonds are not activated in this range, only absorptions of the C-H bonds are observed for E/TFE.

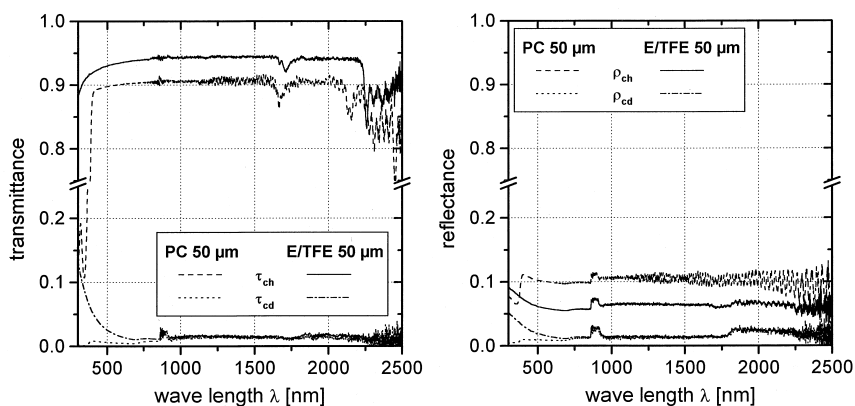


Figure 1. Collimated-hemispherical and collimated-diffuse solar transmittance ( $\tau_{\text{ch}}$ ,  $\tau_{\text{cd}}$ ) and reflectance ( $\rho_{\text{ch}}$ ,  $\rho_{\text{cd}}$ ) spectra for 50  $\mu\text{m}$  thick PC and E/TFE films.

In diffuse transmittance data in Figure 1, differences between the PC and the E/TFE film occur at wavelengths less than 500 nm. These are most likely related to the semi-crystalline morphology of E/TFE versus the amorphous microstructure of PC. Thus, for example it could be shown by AFM experiments that the dimensions of semi-crystalline lamellar band structures in E/TFE are in the range of 60 nm and above, which

corresponds to the increase in  $\tau_{\text{cd}}$  below 500 nm.

For many of the investigated amorphous as well as semi-crystalline films the integral solar extinction coefficients were dominated by scattering. For example, a 50  $\mu\text{m}$  thick E/TFE film shows a solar scattering coefficient of  $6.5 \text{ cm}^{-1}$  and a solar absorption coefficient of less than  $0.1 \text{ cm}^{-1}$ . This indicates that the absorptions in the near infrared have a negligible impact on the solar optical properties. However, for film types with strong absorptions in the near UV range a significant contribution of the solar absorption coefficient to the overall extinction coefficient was found. For example, a 50  $\mu\text{m}$  thick PC film exhibits a solar scattering coefficient of  $3.3 \text{ cm}^{-1}$  and a solar absorption coefficient of  $3.1 \text{ cm}^{-1}$ . In TI structures an incident radiation beam usually passes through successive film elements of the structure (multiple film interaction), before being transmitted through the structure. The strong absorption occurs just at the first film interaction. For subsequent interactions, modified coefficients have to be used which neglect the near UV absorption effect. Taking this into account, average values for subsequent scattering and absorption coefficients (following the first interaction) were calculated neglecting the range of strong absorption during the first radiation/film interaction in the transmittance spectrum. This procedure yields  $\sigma^S$  and  $\kappa^S$  values for the 50  $\mu\text{m}$  thick PC film of 2.8 and less than  $0.1 \text{ cm}^{-1}$ , respectively. In the following, only the solar optical properties neglecting the near UV absorption effect will be described and discussed for film types with significant near UV absorption (e.g., PC, PET, PSU, PEI and PEEK). By this way, only the solar scattering coefficients have to be considered.

Based upon the considerations and the procedure just described, the effect of film thickness,  $d$ , on the solar optical thickness, which is defined as  $\sigma^S * d$ , is shown for several low and high temperature, amorphous and semi-crystalline polymer films in Figure 2. It can be seen that the solar optical thickness of the polymer films investigated ranges from 0.01 to 0.08. Apart from the semi-crystalline F/EP and PET films, which compare well with amorphous polymer films, the semi-crystalline polymer films in general reveal a higher degree of scattering.

For many of the investigated polymer film types, to a good approximation the film thickness dependent solar optical thickness data could be fitted linearly. Thus, it is possible to differentiate between scattering occurring at the film surface and in the bulk (surface vs. volume scattering). The fraction of volume scattering for 50  $\mu\text{m}$  thick films

is expressed by the parameter  $x_v$ . For the amorphous film types it was found that only about 10 % of scattering occurs in the bulk. Even, for many of the semi-crystalline polymer films investigated, still 50 % of scattering can be attributed to surface scattering. Thus, further investigations using atomic force microscopy in an appropriate bandpass were performed to study the influence of surface morphology on the solar optical thickness of transparent polymer films. In this paper the correlation between the solar optical thickness and quantitative parameters describing rough surfaces, the root-mean-square roughness,  $\sigma$ , and the lateral correlation length,  $\xi$ , will be described and discussed in the following. Further details to the calculation procedure for the determination of the quantitative roughness parameters and to the surface morphology of the investigated films are given in ref. [9].

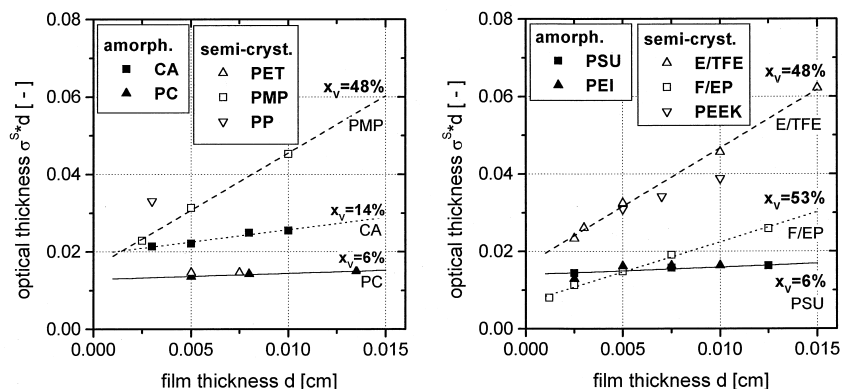


Figure 2. Solar optical thickness ( $\sigma^S \cdot d$ ) of transparent polymer films as a function of film thickness,  $d$  (left: film types with service temperatures of approx. 100 °C; right: high temperature resistant film types) (single film interaction for CA, PMP, PP, E/TFE, F/EP; subsequent film interactions for PC, PET, PSU, PEI, PEEK).

In Figure 3 the root-mean-square (rms) roughness,  $\sigma$ , (left) and the lateral correlation length,  $\xi$ , (right) are plotted versus the solar optical thickness for different amorphous and semi-crystalline films with a thickness of about 50  $\mu\text{m}$ . A reasonable correlation was found between the rms-roughness which is a measure for the vertical fluctuations of roughness and the dimensionless solar optical thickness,  $\sigma^S \cdot d$ . The regression coefficient for the linear fit fixed to the origin was about 0.9. Significant deviations from the linear fit can be observed for polymer films with a low rms-roughness. Probably, these deviations can be attributed to the uncertainties in the determination of the solar optical properties for polymer films with excellent transparency. Furthermore, the

diagram in Figure 3 on the right side shows that there is no significant correlation between the solar-optical thickness and the lateral correlation length which indicates the lateral frequency of roughness fluctuations. Thus, it can be concluded that it is the rms-roughness which determines the solar optical scattering properties of highly transparent polymer films significantly.

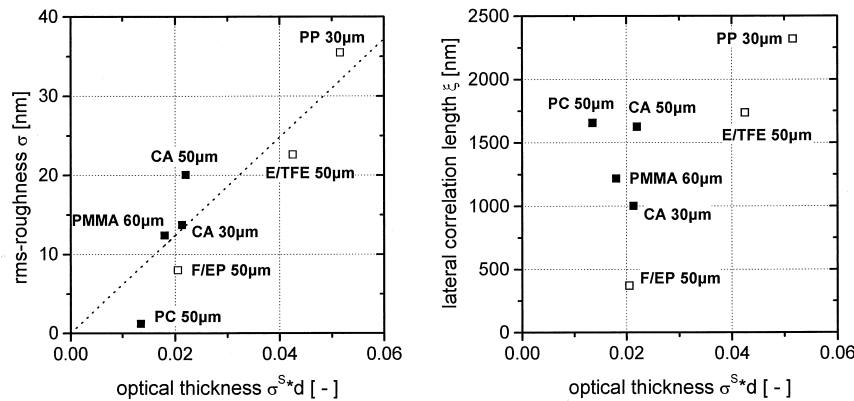


Figure 3. Correlation between the solar optical thickness,  $\sigma^S \cdot d$ , and the root-mean-square roughness,  $\sigma$ , (left) and the lateral correlation length,  $\xi$ , (right) (closed symbols: amorphous films; open symbols: semi-crystalline films).

### Infrared Optical Properties

The collimated-collimated transmittance spectra for 50  $\mu$ m thick PC and E/TFE films are shown over the medium IR range in Figure 4. In addition, the blackbody emissive power function at 20  $^{\circ}$ C is plotted against the wave number. In regions of high transmittance the spectra show the well-known Fabry-Perot interferences. For TI materials in combination with black solar absorbers it is crucial to absorb the infrared radiation as well as possible in order to keep the heat radiation transport low. Thus, especially high absorption is required in the range between 200 and 1500  $\text{cm}^{-1}$ . Both, PC and E/TFE show strong absorption bands in this region. Whereas in PC mainly C-O bonds as well as benzene rings play an important role, in E/TFE the C-F bond is the functional group of major relevance. In addition, imide-, sulfone- and siloxane-groups are important for extinctions in polymers in the medium IR range. Polymers, such as polyolefines (e.g., PP or PMP), which consist of C and H atoms only, reveal the lowest absorption in medium IR range. Furthermore, it should be noticed that below 1000  $\text{cm}^{-1}$ , the maximum of the blackbody emissive power function at 20  $^{\circ}$ C is in this range, mainly polymer specific molecular vibrations contribute to the absorption behaviour.



In Figure 4 it can be further seen, that several of the absorptions for 50  $\mu\text{m}$  films apparently are too strong to be resolved spectrally. Not even for 12.5  $\mu\text{m}$  thick PET or F/EP films, the smallest film thickness investigated, some absorption bands could be resolved. This fact is important for the interpretation of the thickness dependency of the integral infrared absorption.

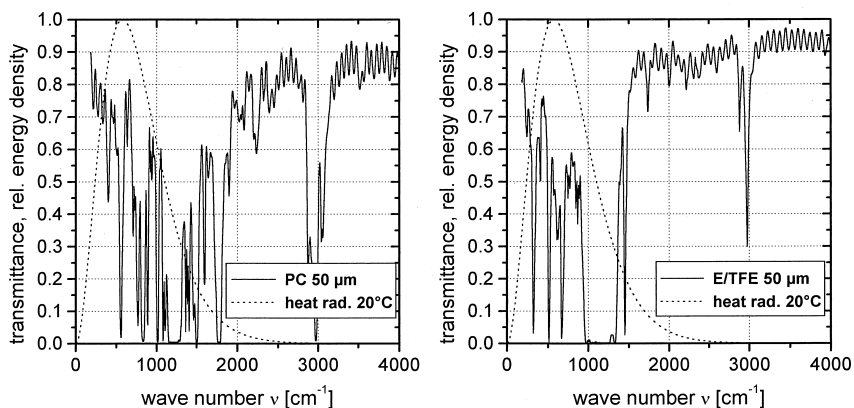


Figure 4. Collimated-collimated infrared transmittance,  $\tau_{cc}$ , spectra for 50  $\mu\text{m}$  thick PC (left) and E/TFE (right) films; in addition, the emissive power function for a blackbody at 20 °C is shown.

In Figure 5 the infrared optical thickness,  $\kappa_{\text{IR}} \cdot d$ , for various polymer films are plotted for low and high temperature polymer films as a function of film thickness. The  $\kappa_{\text{IR}}$  coefficient is an integral value over the range from 180 to 4000  $\text{cm}^{-1}$ . The curves in Figure 5 represent theoretical approximations of the  $\kappa_{\text{IR}} \cdot d$  vs. film thickness dependence, calculated using the transmittance spectrum of 50  $\mu\text{m}$  film as reference. In general, rather good agreement was found between experimental and theoretical curves. The increase of infrared optical thickness (see Figure 5) levels off with increasing film thickness. This is due to the fact that an increase in film thickness does not lead to an enhancement of absorptance at strong absorption bands.

As expected, the lowest infrared optical thicknesses were found for the polyolefines PP and PMP. In contrast, the modified cellulose based polymer CA reveals the highest values for infrared absorption. The high absorption coefficients of CA are predominantly a result of the high density of C-O bonds in the molecular structure of this polymer. While the low temperature polymer film types of PET and PC also contain C-O groups, compared to the cellulose based films their density is significantly lower.

Consequently, with regard to their infrared absorption coefficients, PET, PMMA and PC films were found to be positioned in the midrange between PMP and CA. For 50  $\mu\text{m}$  thick polymer films consisting of C-, O- and H-atoms in the primary structure, a linear correlation between the infrared absorption coefficient and the concentration of C-O groups was found.

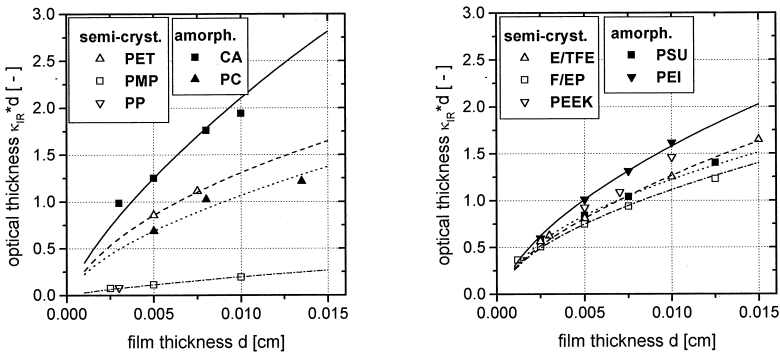


Figure 5. Infrared optical thickness,  $\kappa_{\text{IR}} * d$ , of polymer films with service temperatures of approx. 100 °C (left) and high temperature resistant polymers (right) as a function of film thickness, d.

For the high temperature polymer films shown in Figure 5, the following ranking was obtained: F/EP < E/TFE, PSU < PEEK < PEI. For these films the range covered by the various film types is much reduced due to their molecular architecture. Although different in their chemical nature and in the degree of freedom of mobility, all these polymer types contain a certain density of IR absorbing groups (fluoride, sulphone, ether and imide groups), thus yielding infrared optical thickness values in the upper range of those covered by the low temperature films.

## Conclusions

It has been shown that in the solar wavelength range the non-spectral, solar optical properties of highly transparent polymer films for transparent insulation applications are dominated by scattering occurring mainly at the surface. For various amorphous and semi-crystalline films the root-mean-square surface roughness, a measure for the vertical fluctuations of roughness, correlated well with the solar optical thickness. Concerning high absorbance in the interesting infrared range between 200 to 1500  $\text{cm}^{-1}$  the carbon-oxygen single bond is highly effective for commercial materials with maximum service temperatures of about 100 °C. For 50  $\mu\text{m}$  thick films of PC, PMMA,

PET and CA a good correlation between the concentration of the functional carbon-oxygen group and the non-spectral, infrared optical thickness was found.

- [1] W. J. Platzer, *Solar Energy* **1992**, 49, 359.
- [2] M. Rubin, *Solar Energy Mat.* **1982**, 6, 375.
- [3] J. Pacansky, C. England, R. J. Waltman, *J. Polym. Sci., Polym. Phys. Ed.* **1987**, 25, 901.
- [4] K. G. T. Hollands, K. N. Marshall, R. K. Wedel, *Solar Energy* **1978**, 21, 231.
- [5] J. G. Symons, *J. Solar Energy Eng.* **1982**, 104, 251.
- [6] G. M. Wallner, "Kunststoffe für die transparente Wärmedämmung – Polymerphysikalische Einflüsse und Modellierung", PhD Thesis, University of Leoben, Leoben 2000.
- [7] B. Maheu, J. N. Letoulouzan, G. Gouesbet, *Appl. Opt.* **1984**, 23, 3353.
- [8] A. Haas, "Quantitative Charakterisierung rauher Oberflächen mittels Rasterkraftmikroskopie", Diploma Thesis, University of Leoben, Leoben 1999.
- [9] C. Teichert, A. Haas, G. M. Wallner, R. W. Lang, "Nanometer Scale Characterization of Polymer Films by Atomic-Force Microscopy", in preparation.

